



**HAL**  
open science

## **Robust morris screening method (RMSM) for complex physiological models**

Inès Douania, Jeremy Laforet, Sofiane Boudaoud

### ► **To cite this version:**

Inès Douania, Jeremy Laforet, Sofiane Boudaoud. Robust morris screening method (RMSM) for complex physiological models. *Computer Methods and Programs in Biomedicine*, 2023, 231, pp.107368. <10.1016/j.cmpb.2023.107368>. <hal-04016938>

**HAL Id: hal-04016938**

**<https://utc.hal.science/hal-04016938v1>**

Submitted on 31 Mar 2025

HAL is a multi-disciplinary open access archive for the deposit and dissemination of scientific research documents, whether they are published or not. The documents may come from teaching and research institutions in France or abroad, or from public or private research centers.

L'archive ouverte pluridisciplinaire HAL, est destinée au dépôt et à la diffusion de documents scientifiques de niveau recherche, publiés ou non, émanant des établissements d'enseignement et de recherche français ou étrangers, des laboratoires publics ou privés.



Distributed under a Creative Commons CC BY-NC 4.0 - Attribution - Non-commercial use - International License

# Robust Morris Screening Method (RMSM) for complex physiological models

Ines Douania<sup>a</sup>, Jeremy Laforet<sup>a</sup>, Sofiane Boudaoud<sup>a,\*</sup>

<sup>a</sup>Alliance Sorbonne University, Université de technologie de Compiègne, CNRS, UMR 7338 Biomechanics and Bioengineering, Centre de recherche Royallieu, 60203 Compiègne cedex, France

---

## Abstract

**Background and objectives:** Morris screening sensitivity analysis (MSM) comes forth as the method needing the minimum number of model simulations to qualify the impact of input parameter variations on outputs of complex, nonlinear and overparametrized models. However, the reliability of MSM indices (mean and standard deviation) and the reproducibility of their results are rarely explored despite the input parameter tuning/identification needs. In fact, these models, such those used in medical applications as digital twins, often lie in this category and need efficient and robust tools to assess both sensitivity and reliability of the outputs to numerous input model parameters.

**Methods:** In this study, a new Robust Morris Screening Method (RMSM) is proposed and based on new indices: the absolute median ( $\chi^*$ ) and the median absolute deviation ( $\rho$ ). The proposed RMSM approach is evaluated on a complex multi-scales neuromuscular electrophysiological model simulating HD-sEMG (high density surface electromyography) signals at the skin surface. The reliability and stability of new RMSM indicators are evaluated at different trajectories within the parameter space and compared to classical MSM results. For this purpose, We propose a new methodology for parameter screening based on the ratio  $\rho/\chi^*$  as a graphic indicator of (non)linearity and (non)monotonicity of parameter effects.

**Results:** Firstly, the results demonstrated that the computed elementary effects (EE) of inputs are not normally distributed using MSM indices contrary to the proposed RMSM indices. Secondly, the ranking stability of RMSM indices was earlier obtained from 20 trajectories ( $T=20$ ), while MSM ranking remained unstable until  $T = 100$ . Thirdly, The screening separation between influential and negligible input model parameters was more distinct and interpretable with RMSM than MSM.

**Conclusion:** The proposed RMSM approach ensures a fast, reliable and stable ranking of parameters for complex and overparametrized models compared to classical MSM. this allows a more precise exploration of the model parameter influence space for future application in parameter tuning and identification.

*Keywords:* Neuromuscular model, Sensitivity analysis, Morris method, Reliable indices, Ranking stability

---

\*Corresponding author

Email address: [sofiane.boudaoud@utc.fr](mailto:sofiane.boudaoud@utc.fr) - +(33) 03 44 23 79 29 (Sofiane Boudaoud)

## 1. INTRODUCTION

Models increasingly have a modular and complex design with a large number of inputs [1] and marked by switching between behaviors according to threshold concepts [2]. Model inputs are associated to large uncertainties due to the lack of knowledge and error measurements.

Sensitivity analysis methods are specially useful in these cases to detect modeling assumptions and hypothesis errors, support or exclude some modeling decisions, and reduce model complexity.

However, the selection of an adequate sensitivity analysis method is not trivial. It depends on the model complexity and overparametrization that strongly impacts computation time. Many methods are reported and classified in literature [3] according to these criteria. The two main classes reported are : local methods and global methods [4, 5]. Local approaches study the impact of a small variation around a fixed point of input uncertainty range on the model output(s). These approaches are commonly applied when output have a linear behaviour near a specific nominal value of model inputs, and are not able to assess interactions between parameters. In contrast, global approaches can explore all the input space and interactions between parameters by taking into account computation time. These methods are commonly grouped into derivative-based methods, regression-based methods, qualitative screening methods, and variance-based methods [4, 5]. The results of these methods can be illustrated by: ranking, screening, or mapping. Each representation has a defined utility: Ranking methods are valuable for parameter identification (analytically or numerically); Screening methods can be useful for reducing model complexity; Mapping methods are adapted for studying and understanding model output behavior and at where input space area this output is stable or optimal.

To facilitate the selection of an adequate sensitivity analysis method, a decision tree is proposed by Iooss and Lemaitre (2015)[4]. It suggests the minimum number of model evaluations needed for each method based on the complexity and regularity of the studied system. Most of global sensitivity analysis methods are requiring a large number of model evaluations[4, 5]. Thus, performing these sensitivity analysis methods with complex and high computation time models can be costly.

However, based on this decision tree, the Morris Screening Method (MSM) [6] come forth as the method needing the minimum number of model evaluations for complex, non-regular and/or non-linear ones. It is widely adopted by model makers in many fields (with hundreds of citations in each): Environmental sciences, chemical engineering, Energy, Earth sciences[7, 8, 9, 10]. It screens the most and least sensitive parameters with the fewer number of model simulations and can be considered as semi-quantitative method regarding the information given for interactions between parameters. The MSM varies one input at a time and computes the elementary effect of this variation on the system output. This computation is repeated several times for each input by flowing different trajectories in the input space ( $T$  is the number of trajectories monitored for each input). The mean and the standard deviation of elementary effects (EE) for each input are considered as MSM indices. The input impact is assessed based on the values and ranking of these two indices and the representation of EE distribution by a gaussian.

However, the reliability of MSM indices and the robustness of its results are rarely explored in the literature

especially for complex, nonlinear, multi-scales and multiphysics models [11, 12, 13, 14]. In fact, The mean and standard deviation are not the best suited descriptors for observed non-normal data distributions for these models. Furthermore, most of studies applying MSM have not verified the normality condition on the EE distributions, and these few studies investigating MSM indices [11, 12, 13, 14] have not proposed alternative indices. Indeed, the stability of MSM results is not often assessed by users despite its importance for future parameter identification applications. Also, the setting of the number of trajectories (T) needed for a stable ranking is not argued in most of studies. To fix the variable T, in almost all cases, the authors refer to (Saltelli 2008)[5] and simply use the default recommended value (T=10). For medical applications, this global situation is critical making more difficult the design of reliable physiological models dedicated to Model Aided Diagnosis (MAD).

In this study, we propose a Robust Morris Screening Method (RMSM) approach as an effective methodology to deliver reliable, stable and reproducible parameter ranking results in a minimum computation time. The proposed RMSM approach is evaluated on a recent complex multiphysics and multi-scales neuromuscular model [15, 16] as illustration. This model simulates surface electrical activity of Biceps Brachii muscle during isometric contractions. It features 35 inputs (parameters), 64 HD-sEMG signals and associated computed descriptors as outputs, a complex design, in a high computation time. A comparison is done with the classical MSM. Obtained results are discussed under the scope of future applications in model parameter tuning and identification.

<b>Nomenclature</b>	
<b>Abreviation</b>	<b>Variable and indices</b>
<i>EE</i> Elementary Effects	$\chi^*$ absolute median of EE
<i>MSM</i> Morris Screening Method	$\mu^*$ absolute mean of EE
<i>RMSA</i> Root Mean Square of Amplitude	$\rho$ median absolute deviation of EE
<i>RMSM</i> Robust Morris Screening Method	$\sigma$ standard deviation of EE

## 2. MATERIALS AND METHODS

### 2.1. Robust Morris Screening Method (RMSM)

#### 2.1.1. New sensitivity indices

The MSM method is based on the discretization of variation ranges of inputs into  $l$  levels at where each input is varied while fixing the rest. This process is known as One At a Time design (OAT). Then, the

elementary effect of this variation on the model output is computed by the following equation:

$$EE_{jk} = \frac{y_k(X_1, \dots, X_j + \Delta, \dots, X_n) - y_k(X_1, \dots, X_j, \dots, X_n)}{\Delta} \quad (1)$$

Where,  $EE_{jk}$  is the elementary effect of input  $j$  on the  $k^{th}$  model output,  $\Delta$  is a predetermined perturbation factor of  $X_j$ ,  $y_k(X_1, X_2, \dots, X_j, \dots, X_n)$  is the scalar model output evaluated at inputs  $(X_1, X_2, \dots, X_j, \dots, X_n)$ , while  $y_k(X_1, X_2, \dots, X_j + \Delta, \dots, X_n)$  is the scalar output corresponding to a  $\Delta$  changes in  $X_j$ , and  $n$  is the total number of inputs.

To obtain a reliable impact of inputs, Morris suggests to repeat computation of  $EE_{jk}$  for each input several times [6]. At each time, the input changes its value in a new configuration inside the input space. This configuration is known as the trajectory. Trajectories respect the one at a time design: only one input can change its value through levels  $l$  by jumping only by one step  $\Delta$  at each time. The step  $\Delta$  depends of  $l$ . The total number of points for each trajectory is equal to  $n + 1$ . The total number of trajectories needed to evaluate elementary effect of each input is defined as  $T$ . The mean ( $\mu$ , equation 2) and the standard deviation ( $\sigma$ , equation 3) of all elementary effects (EE) for each input over its  $T$  trajectories are proposed as MSM indices by Morris [6].

$$\mu_{jk} = \frac{1}{T} \sum_{i=1}^T EE_{jk} \quad (2)$$

$$\sigma_{jk} = \sqrt{\frac{1}{T} \sum_{i=1}^T (EE_{jk} - \mu_{jk})^2} \quad (3)$$

The mean  $\mu$  assesses the input influence on the model output. The  $\sigma$  estimates possible non-linear effect and/or interactions between inputs. However, for non monotonic and non-linear models, the distribution of elementary effects can contains positive and negative elements. In this case, the  $\mu$  cannot give an exact impact of inputs due to the sign effect of EE. Campolongo et al. (2007) suggests the use of EE absolute values ( $\mu^*$ , equation (4)) as a reliable and complement MSM indicator [17].

$$\mu_{jk}^* = \frac{1}{T} \sum_{i=1}^T |EE_{jk}| \quad (4)$$

The MSM rationale is to give two approximate indicators quantifying and qualifying a set of elementary effects (EE). Mathematically, the two indicators are the expectation of EE ( $\mu = \mathbb{E}(EE)$ ) and its dispersion ( $\sigma^2 = var(EE)$ ). The original MSM performs the mean as estimator of  $\mu$  and the root mean square deviation as estimator of  $\sigma^2$  (equations (2) and (3)). Statistically, these two indices/estimators gives a reliable characterization of a Laplace-Gaussian distribution. Where the mean ( $\mu$ ) is an unbiased estimator of the expectation, and ( $\sigma^2$ ) is asymptotically unbiased estimator of dispersion/variance (biased for small set of

data). However, the symmetry and Gaussianity of EE distributions are not evident for complex and over-parametrized models. In addition, with MSM method, it is common to compute indices from small samples (small  $T$ ). As consequence, the credibility of  $\mu$  and  $\sigma^2$  cannot be established.

Few studies have investigated the robustness of MSM indices ( $\mu^*$  and  $\sigma$ ), that are efficient only for normal or significantly normal data [18]. Campolongo et al. (2007) [17] have underlined that more robust indicators should be investigated, and have suggested to apply, without demonstration, a new ones based on EE distribution shapes introduced by Hampel (1974) [19]. Memberg et al. (2016) [11] have proposed and applied  $\chi^*$  in the computation of EE average. Thus, Memberg et al. have demonstrated the robustness of  $\chi^*$  against  $\mu^*$  to reproduce a stable ranking [11]. However, they have not proposed a new indicator for EE dispersion quantification. For that reason, they have conserved the original formalism of screening analysis proposed by Morris (1994) [6].

In this study, we propose new indices more adapted to asymmetric and non Gaussian sample distribution: the absolute median ( $\chi^*$ , equation (5)) and the median absolute deviation ( $\rho$ , equation (6)). These two indices are more robust to extremely high and low outliers values and more efficient for non-normal shapes of EE distributions often observed in multi-input and nonlinear models.

$$\chi_{jk}^* = |EE_{jk}|_{(T+1)/2} \quad (5)$$

$$\rho_{jk} = (|EE_{jk}| - \chi_{jk})_{(T+1)/2} \quad (6)$$

### 2.1.2. Reproducibility of RMSM indices ranking

The RMSM requires  $T*(n+1)$  model evaluations, where  $n$  is the number of inputs. The variable  $T$  have an important impact on the computation cost: high value of  $T$  increases the computation time, where too small value can gives wrong input impact evaluation. In this study, we keep the original MSM design (sampling strategy), and we investigate the stability of RMSM indices through eight scales of  $T$ : from 10 to 100. The purpose is to define at which value of  $T$  the stability and reproducibility are guaranteed. In particular, the minimum value of  $T$  needed for reliable and convergent indices is scrutinized. Table 1 summarizes the total number of model simulations needed for each trajectory  $T$  and the corresponding computation time. We should note that MSM and RMSM run with same computing conditions since they use the same sampling strategy of the input space and the same calculator (workstation: 24 cores, Intel Xeon Platinum 8160 X7542, 2.1 Ghz, 1 To RAM). Method indices are computed afterwards.

The stability is assessed with: 1) an individual ranking of parameters using MSM and RMSM indices, and 2) a ranking by group of parameters sharing the same influence/effect.

1. For individual ranking, the stability is evaluated with a numerical position factor as proposed in [20]:

$$PF_{T_i \rightarrow T_j}^{\{\mu^*, \chi^*\}} = \sum_{p=1}^p \frac{|R_{r,i}^{\{\mu^*, \chi^*\}} - R_{r,j}^{\{\mu^*, \chi^*\}}|}{\{\mu^*, \chi^*\}_{R_{p,i} R_{p,j}}} \quad (7)$$

Where  $R_{r,i}$  and  $R_{r,j}$  are the position/ranking of parameter  $p$  at  $T_i$  and  $T_j$  respectively, and  $\{\mu^*, \chi^*\}_{R_{p,i} R_{p,j}}$  is the ranking average of parameter  $p$  obtained by  $T_i$  and  $T_j$  with MSM or RMSM method. The position factor  $PF_{T_i \rightarrow T_j}^{\{\mu^*, \chi^*\}}$  evaluates the ranking changes of all parameters between two different trajectories for MSM or RMSM indices ( $\mu^*$  and  $\chi^*$  respectively). In fact, low value of  $PF_{T_i \rightarrow T_j}^{\{\mu^*, \chi^*\}}$  indicates a small ranking variation between  $T_i$  and  $T_j$ . Furthermore, normalizing by the average rank obtained for  $p$  in  $T_i$  and  $T_j$ :  $\{\mu^*, \chi^*\}_{R_{p,i} R_{p,j}}$  reduces the position changes of negligible parameters. As consequence, the smallest obtained  $PF_{T_i \rightarrow T_j}$  with a posterior stable values, indicates that  $T_j$  is the minimum trajectory needed for convergent and reliable indices.

2. To evaluate the stability of ranking by group of parameters sharing the same impact on the model output, we decide to perform the ranking task according to the influence threshold concept. Thresholds are fixed to define from which value of MSM and RMSM indices the impact of each input is considered important or not. To define this concept, we have fixed the following thresholds : (i) The input is considered in influential group if its EE average varies more than 20% of the model output ( $\chi^* > 20\%$ ,  $\mu^* > 20\%$ ), or the dispersion of its EE is bigger than this value ( $\rho > 20\%$ ,  $\sigma > 20\%$ ), or both. (ii) If  $\chi^*$  or  $\rho$  and respectively  $\mu^*$  or  $\sigma$  have values causing less than 5% of output variation: the input is considered with negligible effect (non-influential group), (iii) parameters situated between these values (5% and 20%) are classified in the intermediate impact group. After, we test the stability of indices by increasing  $T$  values.

Table 1: Computation time and number of model evaluations needed for each  $T$ . The computation time was obtained using 32 parallel processes (workstation: 2ÄÜ24 cores, Intel Xeon Platinum 8160 X7542, 2.1 Ghz, 1 To RAM).

Number of trajectories ( $T$ )	Number of model evaluations	Computation time (32 parallel processes)
10	360	03h25min
20	720	06h02min
30	1080	10h49min
40	1440	15h40min
50	1800	20h28min
60	2160	25h54min
80	2880	37h39min
100	3600	42h35min

### 2.1.3. Reliability of RMSM indices

Classically, MSM users apply the ratio  $\sigma/\mu^*$  to define linearity and monotonicity of input impacts as introduced by Garcia Sanchez et al. (2014) [21]. Since, it was used by the majority of studies applying MSM. In this study, we evaluate the reliability of this ratio with new RMSM indices. Based on normal distribution statistics, authors in [21] estimate that  $\sigma/\mu^*$  is an indicator of almost linear effects (if  $< 0.1$ ) or monotonic effects (if  $< .5$ ). To define linearity and monotonicity of parameter effects with RMSM indices, we propose to perform the following steps:

1. Test the normality of EE distributions around  $\chi^*$  and  $\rho$ . We have performed a Kolmogorov-Smirnov non parametric goodness-of-fit test in the present study [22, 23].
2. Given that EE distributions are normal, we use the statistical property: 95% of EE are within a range  $\chi_r^* \pm 1.96\rho_r$ , to define (non)linearity and (non)monotonicity of EE as justified below:
  - If  $\rho_r/\chi_r^* < 0.1$ : most EE are in a range  $\pm 20\%$  around  $\chi^*$  (Fig. 1 : 95% of EE values are within  $\chi_r^* \pm 1.96 * 0.1\chi_r^* \approx \chi_r^* \pm 0.2\chi_r^*$ ). As consequence, most EE can be considered as constant and the input  $r$  has an almost linear effect (linear effect when  $\rho_r/\chi_r^* = 0$ ).
  - If  $\rho_r/\chi_r^* < 0.5$ : 95% of EE are within  $\chi_r^* \pm 2 * 0.5\chi_r^* = \chi_r^* \pm \chi_r^*$  which is always positive. As consequence, most EE have the same sign (monotonic effect of input  $r$ ).

By applying these assumptions, we can use the ratio  $\rho_r/\chi_r^*$  as graphic indicator of (non)linearity and (non)monotonicity of EE in the input screening with RMSM.

## 2.2. The electrophysiological neuromuscular model

The RMSM performances are evaluated on a recent bio-reliable model of the neuromuscular system simulating the electrical activity recorded at skin surface during isometric contractions of a striated muscle [15, 16]. The model simulates the generation and the propagation of muscle electrical activity through a three-layered conductor volume composed of muscle, adipose tissues, and skin. The muscle activation is driven by a realistic neural command through motor unit recruitment and stochastic neural firing [24]. The recording channels are simulated as a high-density electrode system allowing the generation of 64 HD-sEMG signals from the skin surface allowing several applications [25]. This model contains sub-models [15, 16] simulating the current source (motor units: motoneuron and fibers) generation, the current propagation through a multilayer conductor volume, and the associated muscle anatomy and physiology for a specific muscle contraction level (expressed as percentage of Maximum Voluntary Contraction -MVC) and duration.

### 2.2.1. Model parameter inputs

The electrophysiological neuromuscular system involves 35 input parameters. They describe complex underlying processes related to biocurrent generation and propagation, muscle anatomy and physiology and neural control [15, 16]. The uncertainty ranges of these input parameters are defined according to literature values (Table 2). Information concerning exact values for almost of these parameters is uncertain due to the

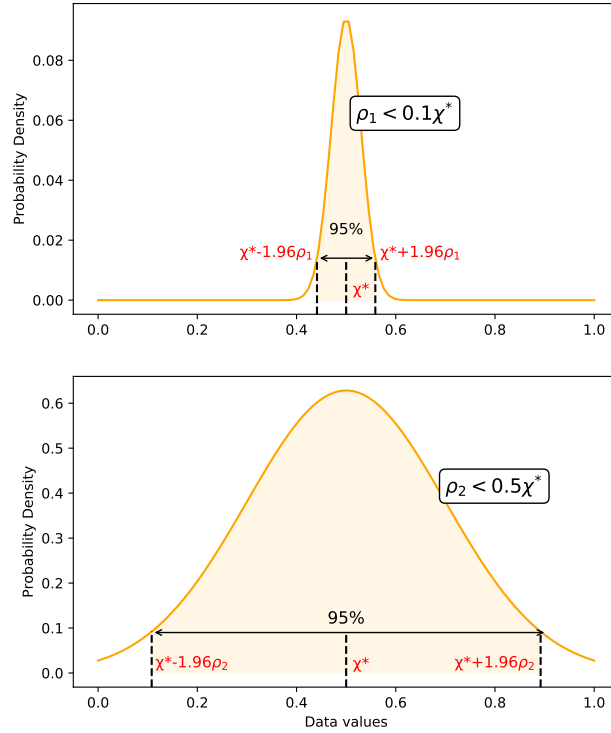


Figure 1: The shape of EE probability density function according to the ratio  $\rho_r/\chi_r^*$ . If  $\rho_r/\chi_r^* < 0.1$ : Parameter have a linear effect on the model output. If  $\rho_r/\chi_r^* < 0.5$ : parameter have a monotonic effect on the model output.

complexity of muscle anatomy and physiology, the inter-subject variability, and the experimental difficulty for precise measurement or reduced uncertain range. One can note also a critical lack in the standardization of experimental setup followed in the literature.

### 2.2.2. Model outputs

The main raw output of the model is the 64 HD-sEMG signals. In order to correlate these signals to the physiological and anatomical muscle properties, many features are extracted from these raw signals [25]. These features are considered as the actual model outputs. For illustration purposes, one classical feature is considered in this study: the mean root mean square of the amplitude (RMSA) among the 64 HD-sEMG signals computed over the 5 seconds of simulated contraction time [25]. Other features will be studied in future studies.

## 3. RESULTS

To properly evaluate the reliability of the sensitivity analysis results using both classical MSM and RMSM, we will: (1) test the normality of the elementary effect distributions according to MSM indices, (2) test the stability and reproducibility of indices when increasing  $T$  values, (3) and compare between MSM and RMSM results according to these two previous criteria.

### 3.1. Elementary effect distributions

To investigate the reliability of MSM indices in parameter ranking, we analyze the elementary effects (EE) distributions. The Fig. 2 describes the EE distributions of the 35 parameters involved in the neuromuscular model. The EE values are computed on the RMSA output at  $T = 30$ . It shows that many input histograms are marked by a skewed and non continuous EE distributions (e.g., diameter of fast intermediate fibers ( $FI_{fD}$ ), the neuromuscular junction position ( $NMJ_{pos}$ )). However, visually, we cannot claim if EE values are normally (or not) distributed around MSM indices ( $\mu^*$  and  $\sigma$ ).

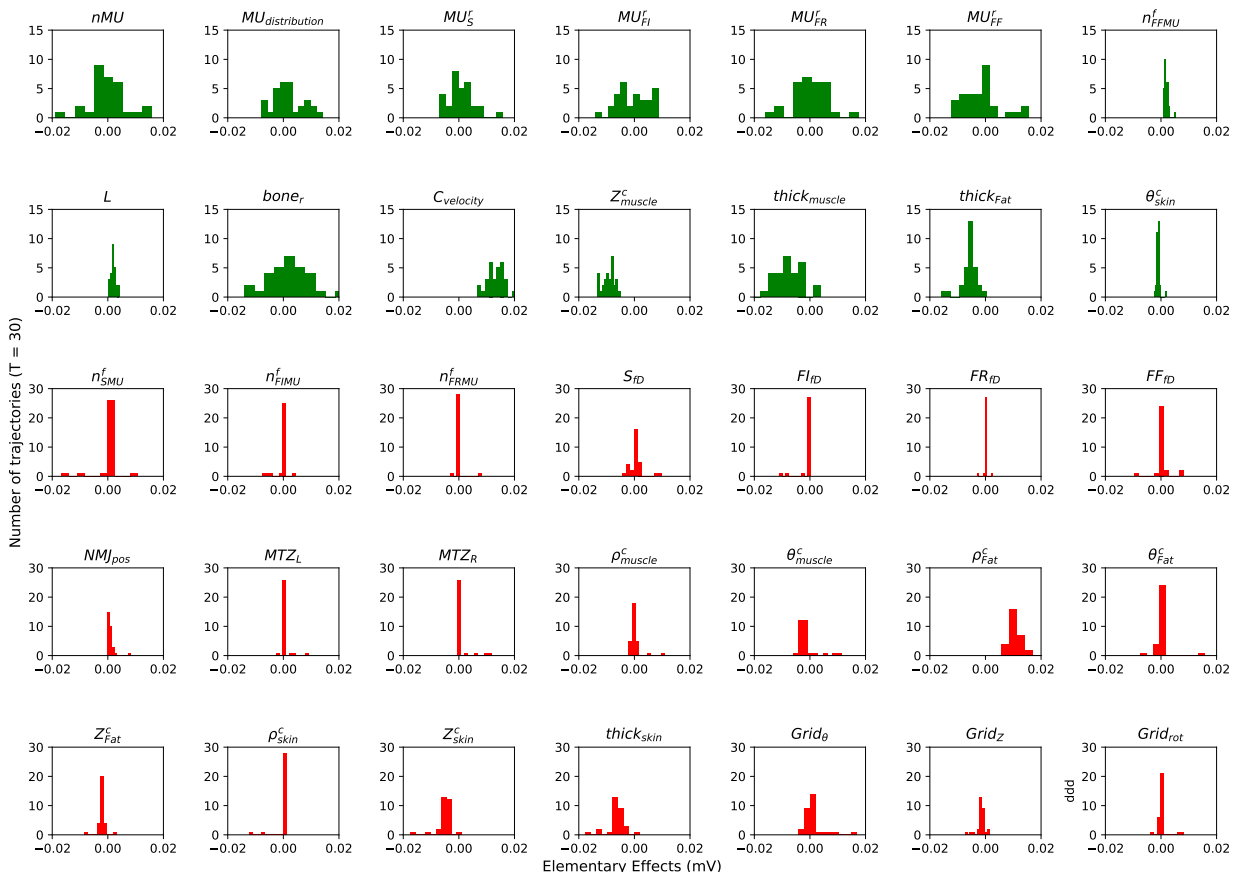


Figure 2: The EE distributions of 35 parameters featured in the neuromuscular model.  $T = 30$ , output = RMSA. Green color: significantly normal EE distributions around  $(\mu^*, \sigma)$ . Red color: non-normal EE distributions around  $(\mu^*, \sigma)$ . Normality test is preformed by Kolmogorov-Smirnov test ( Table 3).

To perform a reliable normality investigation of EE data sets, the Kolmogorov-Smirnov test is applied [22]. The test compares between EE distribution of each input and a theoretical fitted normal distribution generated using the average and dispersion estimators of this input elementary effects [22]. A distribution is considered normal or significantly normal:  $N(\mu^*, \sigma)$  or  $N(\chi^*, \rho)$ , if  $p$ -value  $> 0.05$  (default value of the level of significance).

The Table 3 shows the results of performing the Kolmogorov-Smirnov normality test on EE distributions for MSM and RMSM methods at  $T = 30$ . We observe that EE are not normally distributed around  $\mu^*$  and  $\sigma$  for

many inputs (red color). In contrast, all inputs have a normal distribution around  $\chi^*$  and  $\rho$  using the same test (green color). As consequence, the (non)linearity and (non)monotonicity of parameter effects according to MSM indices are not reliable in agreement with the results of Kolmogorov-Smirnov test for the studied model inputs.

For RMSM indices, as aforementioned in the section 2.1.3, we can define these aspects according to  $\rho/\chi^*$  ratio. The new RMSM screening is proposed in this study with three impact zones: (1) linear effects for parameters with  $\rho/\chi^* < 0.1$ , (2) monotonic effects for parameters with  $\rho/\chi^* < 0.5$ , (3) non-linear and/or non-monotonic effects with possible interactions between parameters ( $\rho/\chi^* > 0.5$ ).

### 3.2. Evaluation of MSM and RMSM indices ranking stability

The ranking stability is investigated by performing the analysis with increased numbers of trajectories (eight steps from  $T = 10$  to  $T = 100$ ) to identify the minimum  $T$  needed for a stable ranking for both MSM and RMSM methods. For individual ranking, parameters are sorted in ascending order from 1 to 35 (total number of parameters) according to  $\mu^*$  for MSM and  $\chi^*$  for RMSM. Parameter with highest  $\mu^*$  or  $\chi^*$  (highest effect on the model output) is ranked number one for both. Conversely, parameter with the most negligible effect on the model output (lower value of  $\mu^*$  or  $\chi^*$ ) is ranked number 35.

The parameter ranking is evaluated at each trajectory  $T: \{10, 20, 30, 40, 50, 60, 80, 100\}$ . To evaluate changes between rankings when increasing  $T$ , the position factors are computed for each pair of trajectories using the equation (7). The table 4 and Fig. 3 show the resulting position factor ( $PF_{T_i \rightarrow T_j}$ ) values and behavior obtained for each pair of trajectories with: (a) MSM indices, and (b) RMSM indices. We observe that from low number of trajectories with RMSM (from  $T = 30$ ), the  $PF_{T_i \rightarrow T_j}^{\chi^*}$  values remain stable and lower than MSM ( $PF_{T_{80} \rightarrow T_{100}}^{\mu^*} > PF_{T_{30} \rightarrow T_{40}}^{\chi^*}$ ). In fact, low values of  $PF$  indicate that most of the parameters remain nearly in the same ranking position between two successive trajectories. Therefore, according to table 4 and Fig. 3, values of  $T$  above 30 provide a suitable estimation of sensitivity measures with RMSM indices. This is not the case for MSM, where ranking variability remains over 30.

Furthermore, in order to efficiently evaluated the input parameter effects, we have performed a ranking by group of parameters sharing the same impact on the model output. We have fixed effect thresholds based on MSM and RMSM indices as outlined in 2.1.2: (1) influential group including parameters with EE average and/or dispersion causing more than 20% of the model output ( $(\chi^*, \rho) > 20\%$ ,  $(\mu^*, \sigma) > 20\%$ ), (2) non-influential group with parameters causing less than 5% of output variation ( $(\chi^*, \rho) < 5\%$ ,  $(\mu^*, \sigma) < 5\%$ ), and (3) intermediate group of parameters located between the two previous groups.

The Fig.4(a) illustrates a screening sensitivity analysis of the studied neuromuscular model with the MSM method at  $T = 30$  and using classical  $\mu^*$  and  $\sigma$  indices. As mentioned before, the model output is the mean RMSA of HD-sEMG signals measured at the skin surface by the 64 electrodes. The sensitivity analysis space is divided into four zones according to the ratio  $\sigma/\mu_r^*$  classification suggested in [21]. For clarity, each group of inputs is marked by a defined color and marker according to its influence level. Thresholds separating influential zones are marked by dashed lines. Elementary effects have the same unit as the model output:

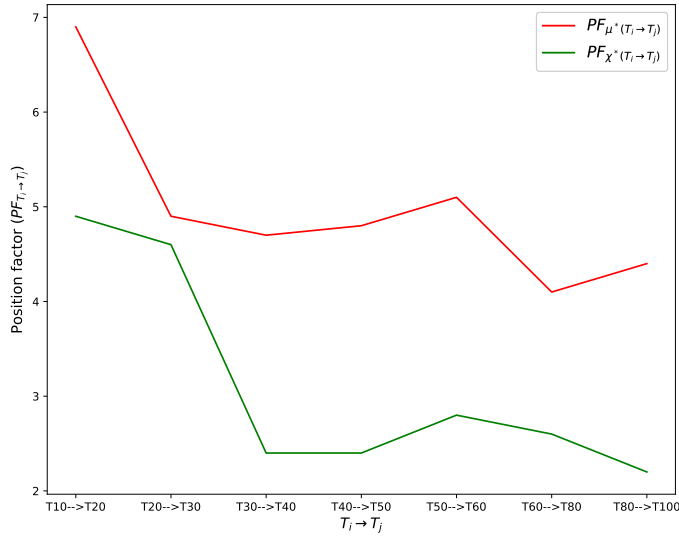


Figure 3: The position factors  $PF_{T_i \rightarrow T_j}$  values and behavior obtained for each pair of trajectories with MSM indices (red color), and RMSM indices (green color).

mV. The stability of this approach is observed in Fig.4(b) at different trajectories  $T$ .

The Fig.5(a) illustrates a screening sensitivity analysis with the RMSM method at  $T = 30$  with the same model output and with the same colors and markers for influential groups. The stability of the RMSM indices is observed in Fig.5(b) at different trajectories  $T$ .

We observe that the RMSM guarantees the stability and reproducibility of parameter ranking from  $T = 20$  (Fig. 5(b)). A small  $T$  value reduces significantly the computation time of the sensitivity analysis. The minimum number of model evaluations needed to perform a sensitivity analysis at  $T = 20$  is 720, computed in  $6h02min$  (Table 1).

In contrast, the Fig. 4(b) shows that parameter ranking remains unstable until  $T = 100$  with MSM method (the computation time is equal to  $42h35min$ ). In this figure, we observe many disruptions in the ranking for many inputs, e.g., the parameter  $\theta_{skin}^c$  (angular skin conductivity) varies its ranking from large impact group at  $T = 60$ , to intermediate impact group at  $T = 80$ , to small impact group at  $T = 100$ . This instability distorts the evaluation of parameter impacts when delivering sensitivity analysis results. Furthermore, the linearity and monotonicity of input impacts are attributed for only few parameters with significantly normal EE according to MSM indices (Table 3). Thus, a common attributions/screening of linear and monotonic effects for all parameters as in Fig.4(a) is inconsistent. However, the RMSM indices give a conjoint representation of linear and monotonic zones for all parameters (Fig. 5(a)).

#### 4. DISCUSSIONS

The MSM is one of the rare tools to perform sensitivity analysis for high cost and complex models at the smallest computation time as depicted in the selection decision tree proposed in Iooss and Lemaitre (2015) [4].

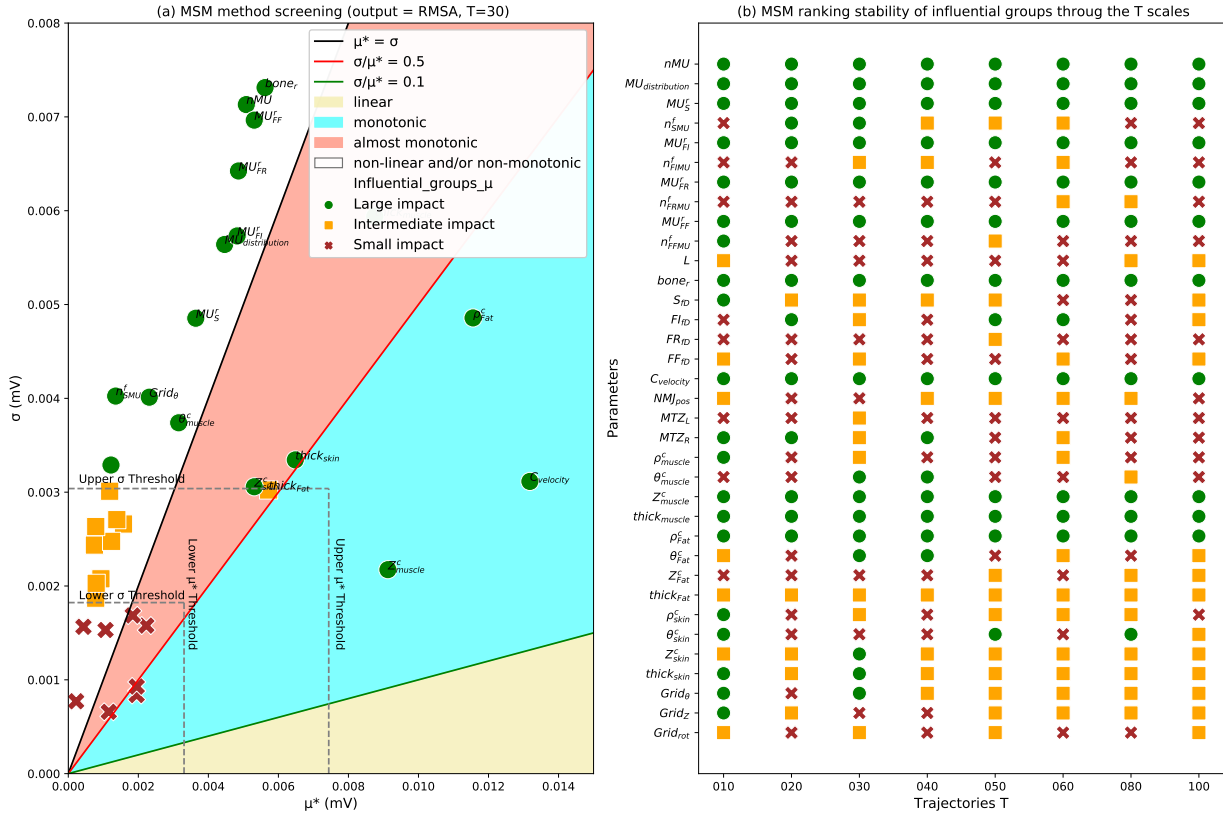


Figure 4: (a) Sensitivity analysis screening with MSM. Output = RMSA of HD-sEMG signals (mV).  $T = 30$ . Three influential groups: low impact (dark red), Medium impact (orange). High impact (green). (b) Ranking stability of MSM method at different trajectories  $T$ .

However, the approach bears on strong normality assumption of the EE distributions and presents unstable results. The present study is motivated by proposing a fast, robust and stable Morris screening sensitivity analysis for high computation cost and complex physiological models. The model, depicted in Carriou et al. (2016) and used in this study, satisfies these criteria [15].

#### 4.1. Selection of appropriate indices: $\chi^*$ and $\rho$

The new RMSM proposes the application of  $\chi^*$  and  $\rho$  as sensitivity indicators: the absolute median and the median absolute deviation respectively. The selection of these indices is based on several studies e.g., [19, 35] for its relevance to non-normal data distributions and its robustness to eliminate outliers causing a wrong estimation of data average and dispersion. The Kolmogorv-Smirnov normality test showed that EE distributions are significantly normal around RMSM indices for all parameters. This was not the case for MSM indices (Table 3). We should note that other alternatives to  $\rho$  exist in the literature and can be applied if the normality of EE distributions is not achieved [36].

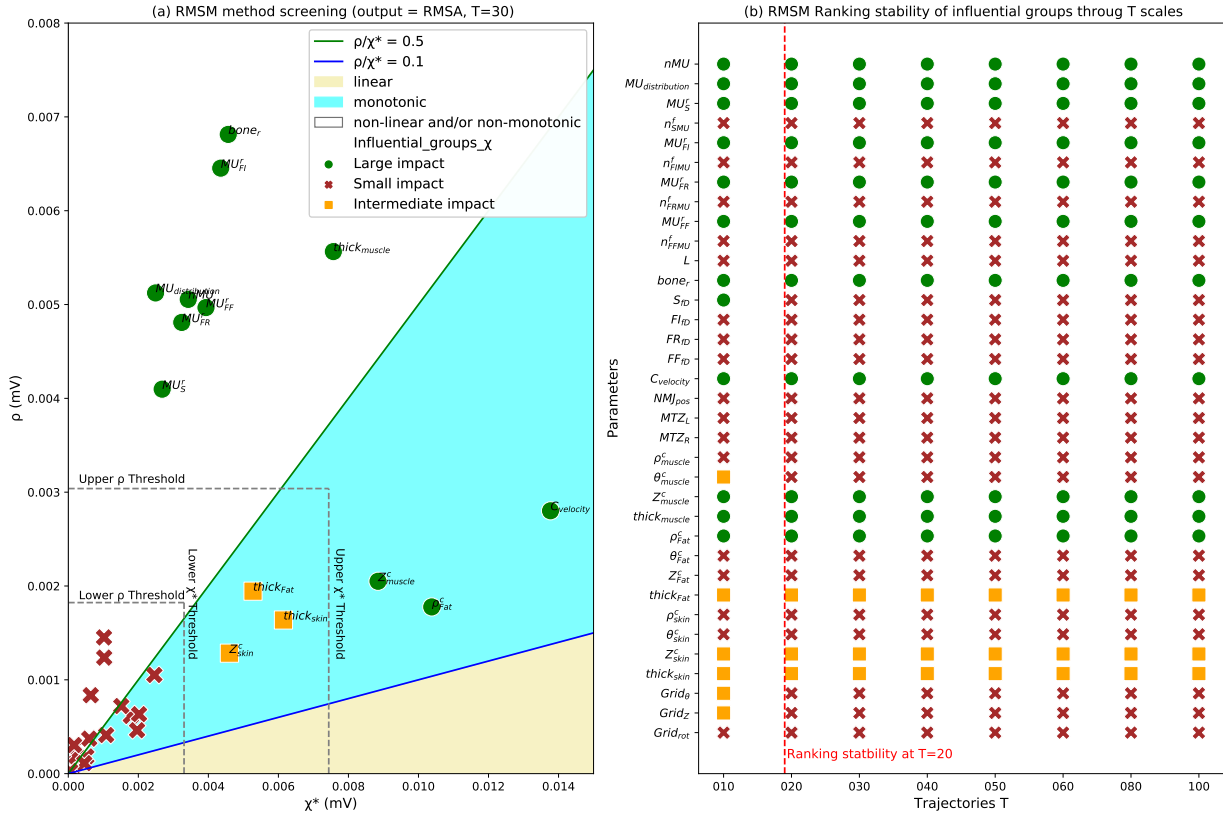


Figure 5: (a) Sensitivity analysis screening with RMSM. Output = RMSA of HD-sEMG signals (mV).  $T = 30$ . Three influential groups: low impact (dark red), Medium impact (orange). High impact (green). (b) Ranking stability of RMSM method at different trajectories  $T$ . The RMSM ranking stability is obtained at  $T = 20$ .

#### 4.2. Linearity and monotonicity evaluation using the $\rho/\chi^*$ ratio

Garcia Sanchez et al. (2014) [21], using the ratio  $\sigma/\mu^*$ , have defined the zone of linear effects, monotonic effects, and non linear effects and/or with interactions between inputs. Their hypothesis is based on: 1) statistical properties of normal EE distributions, 2) equality between the two ratios  $\sigma/\mu^*$  and  $\sigma/|\mu|$  to define the three zones mentioned above for non-normal data. However, This equality cannot deliver the same conclusions with the new RMSM indices. In fact, the equality between  $\rho/\chi^*$  and  $\rho/|\chi|$  means that  $\chi^*$  is equal to  $|\chi|$  but does not mean necessarily that EE have the same sign (eq. 5). To identify the monotonicity and linearity of parameter effects, this study have proposed to use the  $\rho/\chi^*$  ratio. Statistical properties of normal or significantly normal EE distributions (normality test is required), indicated that most EE (95%) have the same sign (monotonic effect) if  $\rho/\chi^*$  is smaller than 0.5, and 95% of EE are constant (linear effect) if  $\rho/\chi^*$  is smaller than 0.1. Such conclusions give the monotonic and linear effects zones as depicted in the Fig.4(a) and Fig.5(a) and presented partially in [21]. In fact, obtained results for MSM on Fig.4(a) showed 12 parameters with large impact (green circle), 9 with low impact (red cross) and the rest with medium impact (orange square). No parameter was found as linear one. One can observe that 6 parameter are monotonic or almost monotonic excluding low impact parameters. The parameter cloud is relatively continuous with no

clear boundaries. Regarding RMSM results depicted on Fig.5(a), we can observe clear boundaries between groups indicating good separability and better reliability. We obtained 11 parameters with large impact (green circle), 21 with low impact (red cross), that are regrouped, and the rest with medium impact (orange square). As for MSM, no parameter was found as linear one. From the studied figure, 6 parameters exhibit monotonic behavior with RMSA (the same as MSM) excluding low impact parameters. Thanks to the good observed separability, the RMSM results are more straightforward than MSM ones.

#### 4.3. Stability analysis of RMSM and MSM indices

The present study also demonstrated the early stability of RMSM indices ranking from  $T = 30$  with individual ranking. For ranking by group of parameters sharing the same influence on the model output (thresholds concept), the RMSM method reduces the minimum  $T$  needed for stable ranking from  $T = 20$  ;  $T = 30$  with individual ranking. In contrast, MSM indices remain unstable until  $T = 100$  (Fig. 4 and 5). As illustration, the skin conductivity parameter jumped across all groups with increasing  $T$  from 60 to 100. It is important to recall that the computation time needed to perform Morris screening analysis for  $T = 20$  and  $T = 100$  are respectively *6h02min* and *42h35min* (Table 1). Yet, 20 trajectories were sufficient to get a stable and robust ranking with RMSM indices for the studied neuromuscular model. Such reduced computing time and ranking stability will be useful for future applications such model parameter ranking where influential model parameter input will be tuned with caution where negligible ones can be fixed to reference values. This will also have a strong impact on experimental setup design. It will allows a focus on these influential parameters and by the way optimized and limited experimental setups in actual more severe regulations context. The proposed linearity and monotonicity analysis will be a mandatory pre-step for parameter identification. In fact, this knowledge will permit the rapid selection of parameter that exhibits one or both properties. This will greatly accelerate/simplify the identification task for noninvasive parameter estimation. In medical applications, an access to physiological parameter hardly obtained noninvasively will open the door to the design of improved medical tools using Model Aided Diagnosis (MAD).

## 5. CONCLUSION

In this study, after recalling the MSM formalism, its usefulness and limitations, we have proposed an improved version, focusing on robustness and reliability, and dedicated to complex physiological and over-parametrized models with high computational cost. In fact, tested on a recent complex eletrophysiological model of the neuromuscular system, the MSM results revealed that parameter rankings, obtained by using the absolute mean value  $\mu^*$  and the standard deviation  $\sigma$  of the elementary effects as a criterion, are unstable and unreliable. The new proposed RMSM guaranteed, according to the obtained results, the satisfaction of these criteria trough parameter ranking stability with optimized computation time according to reduced number of trajectories T. It uses two new robust indices to evaluate elementary effects: the absolute median ( $\chi^*$ ) and the median absolute deviation ( $\rho$ ). By applying a normality test, we showed that elementary effects are

normally distributed for all parameters with RMSM indices  $(\chi^*, \rho)$  in this study. In contrast, many parameters have a non-normal distributions using MSM indices  $(\mu^*, \sigma)$ . As a consequence, the screening information about the linearity, monotonicity, and interactions between parameters provided by MSM are unreliable and distorts the sensitivity analysis results. In fact, this information is based on statistical properties of the ratio  $\sigma/\mu^*$  for normal distributions. Thus, the new RMSM ratio  $\rho/\chi^*$  is more appropriate as a graphic indicator of parameter effect features as observed on the obtained results.

In future studies, the RMSM will allow more precise tuning of model parameters by clearer separation between influential and negligible parameters. For identification purpose, the RMSM will be used to select the best parameter candidates according to linearity and monotonicity. It is envisaged to rapidly reach these objectives for investigating the studied neuromuscular model in a near future.

## 6. Acknowledgment

This work was carried out and funded in the framework of the Labex MS2T. It was supported by the French Government, through the program "Investments for the future" managed by the National Agency for Research (Reference ANR-11-IDEX-0004-02). We thank equally the Region Hauts-de-France for co-funding this work.

## Conflict of interest

The authors have no conflicts of interest to declare that are relevant to the content of this article.

## References

- [1] G. Lee, W. Kim, H. Oh, B. D. Youn, N. H. Kim, Review of statistical model calibration and validation from the perspective of uncertainty structures, *Struct Multidisc Optim* 60 (4) (2019) 1619–1644. doi:10.1007/s00158-019-02270-2.
- [2] D. C. Wynn, P. J. Clarkson, Process models in design and development, *Res Eng Design* 29 (2) (2018) 161–202. doi:10.1007/s00163-017-0262-7.
- [3] G. Qian, A. Mahdi, Sensitivity analysis methods in the biomedical sciences, *Mathematical Biosciences* 323 (2020) 108306. doi:10.1016/j.mbs.2020.108306.
- [4] B. Iooss, P. Lemaître, A review on global sensitivity analysis methods, in: C. Meloni, G. Dellino (Eds.), *Uncertainty management in Simulation-Optimization of Complex Systems: Algorithms and Applications*, Springer, 2015.
- [5] A. Saltelli, *Global Sensitivity Analysis: The Primer* by Andrea Saltelli, Marco Ratto, Terry Andres, Francesca Campolongo, Jessica Cariboni, Debora Gatelli, Michaela Saisana, Stefano Tarantola, *International Statistical Review* 76 (2008) 452–452. doi:10.1111/j.1751-5823.2008.00062\_17.x.

- [6] M. D. Morris, Factorial Sampling Plans for Preliminary Computational Experiments, *Technometrics* 33 (2) (1991) 161–174. doi:10.1080/00401706.1991.10484804.
- [7] Y. Gan, Q. Duan, W. Gong, C. Tong, Y. Sun, W. Chu, A. Ye, C. Miao, Z. Di, A comprehensive evaluation of various sensitivity analysis methods: A case study with a hydrological model, *Environmental Modelling & Software* 51 (2014) 269–285. doi:10.1016/j.envsoft.2013.09.031.
- [8] K. J. Hughes, J. F. Griffiths, M. Fairweather, A. S. Tomlin, Evaluation of models for the low temperature combustion of alkanes through interpretation of pressure–temperature ignition diagrams, *Phys. Chem. Chem. Phys.* 8 (27) (2006) 3197–3210. doi:10.1039/B605379C.
- [9] A. Janse van Rensburg, G. van Schoor, P. A. van Vuuren, Stepwise Global Sensitivity Analysis of a Physics-Based Battery Model using the Morris Method and Monte Carlo Experiments, *Journal of Energy Storage* 25 (2019) 100875. doi:10.1016/j.est.2019.100875.
- [10] M. Jaxa-Rozen, J. Kwakkel, Tree-based ensemble methods for sensitivity analysis of environmental models: A performance comparison with Sobol and Morris techniques, *Environmental Modelling & Software* 107 (2018) 245–266. doi:10.1016/j.envsoft.2018.06.011.
- [11] K. Menberg, Y. Heo, R. Choudhary, Sensitivity analysis methods for building energy models: Comparing computational costs and extractable information, *Energy and Buildings* 133 (2016) 433–445. doi:10.1016/j.enbuild.2016.10.005.
- [12] S. Petersen, M. H. Kristensen, M. D. Knudsen, Prerequisites for reliable sensitivity analysis of a high fidelity building energy model, *Energy and Buildings* 183 (2019) 1–16. doi:10.1016/j.enbuild.2018.10.035.
- [13] S. Sreedevi, T. I. Eldho, C. G. Madhusoodhanan, T. Jayasankar, Multiobjective sensitivity analysis and model parameterization approach for coupled streamflow and groundwater table depth simulations using SHETRAN in a wet humid tropical catchment, *Journal of Hydrology* 579 (2019) 124217. doi:10.1016/j.jhydro.2019.124217.
- [14] M. Awad, T. Senga Kiese, Z. Assaghir, A. Ventura, Convergence of sensitivity analysis methods for evaluating combined influences of model inputs, *Reliability Engineering & System Safety* 189 (2019) 109–122. doi:10.1016/j.ress.2019.03.050.
- [15] V. Carriou, S. Boudaoud, J. Laforet, F. S. Ayachi, Fast generation model of high density surface EMG signals in a cylindrical conductor volume, *Computers in Biology and Medicine* 74 (2016) 54–68. doi:10.1016/j.combiomed.2016.04.019.
- [16] V. Carriou, S. Boudaoud, J. Laforet, Speedup computation of HD-sEMG signals using a motor unit-specific electrical source model, *Medical & Biological Engineering & Computing* 56 (8) (2018) 1459–1473. doi:10.1007/s11517-018-1784-5.

- [17] F. Campolongo, J. Cariboni, A. Saltelli, An effective screening design for sensitivity analysis of large models, *Environmental Modelling & Software* 22 (10) (2007) 1509–1518. doi:10.1016/j.envsoft.2006.10.004.
- [18] J. Miller, Short report: Reaction time analysis with outlier exclusion: Bias varies with sample size, *The Quarterly Journal of Experimental Psychology Section A* 43 (4) (1991) 907–912. doi:10.1080/14640749108400962.
- [19] F. R. Hampel, The Influence Curve and its Role in Robust Estimation, *Journal of the American Statistical Association* 69 (346) (1974) 383–393. doi:10.1080/01621459.1974.10482962.
- [20] M. V. Ruano, J. Ribes, A. Seco, J. Ferrer, An improved sampling strategy based on trajectory design for application of the Morris method to systems with many input factors, *Environmental Modelling & Software* 37 (2012) 103–109. doi:10.1016/j.envsoft.2012.03.008.
- [21] D. Garcia Sanchez, B. LacarriÁre, M. Musy, B. Bourges, Application of sensitivity analysis in building energy simulations: Combining first- and second-order elementary effects methods, *Energy and Buildings* 68 (2014) 741–750. doi:10.1016/j.enbuild.2012.08.048.
- [22] F. J. M. Jr, The Kolmogorov-Smirnov Test for Goodness of Fit, *Journal of the American Statistical Association* 46 (253) (1951) 68–78. doi:10.1080/01621459.1951.10500769.
- [23] M. Aslam, Introducing Kolmogorov’s Smirnov Tests under Uncertainty: An Application to Radioactive Data, *ACS Omega* 5 (1) (2019) 914–917. doi:10.1021/acsomega.9b03940.
- [24] T. I. Arabadzhiev, V. G. Dimitrov, N. A. Dimitrova, G. V. Dimitrov, Influence of motor unit synchronization on amplitude characteristics of surface and intramuscularly recorded EMG signals, *Eur J Appl Physiol* 108 (2) (2009) 227. doi:10.1007/s00421-009-1206-3.
- [25] M. Al Harrach, V. Carriou, S. Boudaoud, J. Laforet, F. Marin, Analysis of the sEMG/force relationship using HD-sEMG technique and data fusion: A simulation study, *Computers in Biology and Medicine* 83 (2017) 34–47. doi:10.1016/j.combiomed.2017.02.003.
- [26] C. Neuwirth, C. Burkhardt, J. Alix, J. Castro, M. de Carvalho, M. Gawel, S. Goedee, J. Grosskreutz, T. Lenglet, C. Moglia, T. Omer, M. Schrooten, M. Weber, Quality Control of Motor Unit Number Index (MUNIX) Measurements in 6 Muscles in a Single-Subject ‘‘Round-Robin’’ Setup, *PLoS One* 11 (5). doi:10.1371/journal.pone.0153948.
- [27] P. O. Eriksson, Muscle-fibre composition of the human mandibular locomotor system. Enzyme-histochemical and morphological characteristics of functionally different parts, *Swed Dent J Suppl* 12 Suppl (1982) 1–44.

- [28] C. S. Klein, G. D. Marsh, R. J. Petrella, C. L. Rice, Muscle fiber number in the biceps brachii muscle of young and old men, *Muscle & Nerve* 28 (1) (2003) 62–68. doi:10.1002/mus.10386.
- [29] H. Haapasalo, H. Sievanen, P. Kannus, A. Heinonen, P. Oja, I. Vuori, Dimensions and estimated mechanical characteristics of the humerus after long-term tennis loading, *Journal of Bone and Mineral Research* 11 (6) (1996) 864–872. doi:https://doi.org/10.1002/jbmr.5650110619.
- [30] P. O. Eriksson, L. E. Thornell, Histochemical and morphological muscle-fibre characteristics of the human masseter, the medial pterygoid and the temporal muscles, *Archives of Oral Biology* 28 (9) (1983) 781–795. doi:10.1016/0003-9969(83)90034-1.
- [31] X. Ye, T. W. Beck, N. P. Wages, Relationship between innervation zone width and mean muscle fiber conduction velocity during a sustained isometric contraction, *Journal of Musculoskeletal & Neuronal Interactions* 15 (1) (2015) 95–102.
- [32] H. G. J. Kortman, S. C. Wilder, T. R. Geisbush, P. Narayanaswami, S. B. Rutkove, Age and gender associated differences in electrical impedance values of skeletal muscle, *Physiol Meas* 34 (12) (2013) 1611–1622. doi:10.1088/0967-3334/34/12/1611.
- [33] S. Gabriel, R. W. Lau, C. Gabriel, The dielectric properties of biological tissues: II. Measurements in the frequency range 10 Hz to 20 GHz, *Phys. Med. Biol.* 41 (11) (1996) 2251–2269. doi:10.1088/0031-9155/41/11/002.
- [34] Y. Ishida, H. Kanehisa, T. Fukunaga, Differences in Muscle Thicknesses of Male and Female Japanese Elite Athletes, *Japanese Journal of Physical Fitness and Sports Medicine* 41 (2) (1992) 233–240. doi:10.7600/jspfsm1949.41.233.
- [35] C. Leys, C. Ley, O. Klein, P. Bernard, L. Licata, Detecting outliers: Do not use standard deviation around the mean, use absolute deviation around the median, *Journal of Experimental Social Psychology* 49 (4) (2013) 764–766. doi:10.1016/j.jesp.2013.03.013.
- [36] P. J. Rousseeuw, C. Croux, Alternatives to the Median Absolute Deviation, *Journal of the American Statistical Association* 88 (424) (1993) 1273–1283. doi:10.1080/01621459.1993.10476408.

Table 2: list of parameters and assigned uncertainty ranges used for the sensitivity analysis.

Parameter	Description	Lower bound	Upper bound	Unit	References
$nMU$	Number of Motor Units	120	220	-	[26]
$MU_{distribution}$	Distribution of MU according to type	S=33 FI=5 FR=14 FF=18	S=48 FI=20 FR=23 FF=40	%	[27]
$MU_S^r$	Radius of MU type S	2.3	2.7	mm	[24]
$n_{SMU}^f$	Number of fiber per MU type S	400	440	-	[28, 26]
$MU_{FI}^r$	Radius of MU type FI	2.8	3.2	mm	[24]
$n_{FIMU}^f$	Number of fiber per MU type FI	90	111	-	[28, 26]
$MU_{FR}^r$	Radius of MU type FR	2.5	3	mm	[24]
$n_{FRMU}^f$	Number of fiber per MU type FR	190	210	-	[28, 26]
$MU_{FF}^r$	Radius of MU type FF	3	3.5	mm	[24]
$n_{FRMU}^f$	Number of fiber per MU type FF	280	300	-	[28, 26]
$L$	Muscle length	115.1	130.6	mm	[25]
$bone_r$	Bone radius	11.7	13.2	mm	[29]
$S_{fD}$	S fibers diameter	64	68	$\mu m$	[30]
$FI_{fD}$	FI fibers Diameter	73	75	$\mu m$	[30]
$FR_{fD}$	FR fibers diameter	74	78	$\mu m$	[30]
$FF_{fD}$	FF fibers diameter	72	76	$\mu m$	[30]
$NMJ_{pos}$	Neuromuscular junction position	0	4	mm	[15]
$C_{velocity}$	Conduction velocity of fibers	2.5	4.8	$m.s^{-1}$	[31]
$MTZ_L$	Left myotendinous length	14	16	mm	[15]
$MTZ_R$	Right myotendinous length	14	16	mm	[15]
$\rho_{muscle}^c$	Radial muscle conductivity	0.4	0.6	$S.m^{-1}$	[32]
$\theta_{muscle}^c$	Angular muscle conductivity	0.4	0.6	$S.m^{-1}$	[32]
$Z_{muscle}^c$	Longitudinal muscle conductivity	0.86	0.99	$S.m^{-1}$	[32]
$thick_{muscle}$	Muscle thickness	40	46	mm	[29]
$\rho_{muscle}^{Fat}$	Radial fat conductivity	0.04	0.07	$S.m^{-1}$	[33]
$\theta_{Fat}^c$	Angular fat conductivity	0.04	0.07	$S.m^{-1}$	[33]
$Z_{Fat}^c$	Longitudinal fat conductivity	0.04	0.07	$S.m^{-1}$	[33]
$thick_{Fat}$	Fat thickness	4	5	mm	[34]
$\rho_{skin}^c$	Radial skin conductivity	0.9	1.2	$S.m^{-1}$	[33]
$\theta_{skin}^c$	Angular skin conductivity	0.9	1.2	$S.m^{-1}$	[33]
$Z_{skin}^c$	Longitudinal skin conductivity	0.9	1.2	$S.m^{-1}$	[33]
$thick_{skin}$	Skin conductivity	0.9	1.2	mm	[32]
$Grid_{\theta}$	Angular grid center	0	5	$^{\circ}$	[15]
$Grid_z$	Longitudinal grid center	15	18	mm	[15]
$Grid_{rot}$	Electrode grid rotation	0	10	$^{\circ}$	[15]

Table 3: The results of Kolmogorov-Smirnov normality test applied on elementary effects data of each parameter, and according to MSM and RMSM indices at  $T = 30$ . The  $p$  values  $> 0.05$  indicate that EE data is significantly normal (green color).

Parameters	p value (MSM, T=30)	p value (RMSM, T=30)
$nMU$	0.48	0.954
$MU_{distribution}$	0.8118	0.656
$MU_S^r$	0.9945	1
$n_{SMU}^f$	7.43e-06	0.811
$MU_{FI}^r$	0.9107	0.925
$n_{FIMU}^f$	1.27e-05	0.632
$MU_{FR}^r$	0.5864	0.736
$n_{FRMU}^f$	1.05e-06	0.448
$MU_{FF}^r$	0.4159	0.762
$n_{FFMU}^f$	0.5493	0.949
$L$	0.6869	0.448
$bone_r$	0.9908	0.892
$S_{fD}$	3.59e-02	0.432
$FI_{fD}$	5.01e-07	0.632
$FR_{fD}$	1.28e-05	0.996
$FF_{fD}$	6.20e-04	0.384
$C_{velocity}$	0.8885	0.627
$NMJ_{pos}$	1.36e-02	0.441
$MTZ_L$	4.08e-05	0.866
$MTZ_R$	3.44e-06	0.632
$\rho_{muscle}^c$	4.96e-03	0.07
$\theta_{muscle}^c$	4.02e-03	0.402
$Z_{muscle}^c$	0.6422	0.937
$thick_{muscle}$	0.976	0.869
$\rho_{Fat}^c$	4.69e-02	0.436
$\theta_{Fat}^c$	8.54e-07	0.728
$Z_{Fat}^c$	3.19e-02	0.901
$thick_{Fat}$	0.2454	0.774
$\rho_{skin}^c$	5.22e-08	0.108
$\theta_{skin}^c$	0.0948	0.564
$Z_{skin}^c$	4.42e-02	0.335
$thick_{skin}$	4.39e-02	0.548
$Grid_{\theta}$	8.13e-03	0.528
$Grid_Z$	3.06e-02	0.759
$Grid_{rot}$	2.44e-05	0.91

Table 4: Computed position factors  $PF_{T_i \rightarrow T_j}$  according to (a)  $\mu^*$  (MSM) ranking; (b)  $\chi^*$  (RMSM) ranking .

$PF_{T_i \rightarrow T_j}$	$T_{10} \rightarrow T_{20}$	$T_{20} \rightarrow T_{30}$	$T_{30} \rightarrow T_{40}$	$T_{40} \rightarrow T_{50}$	$T_{50} \rightarrow T_{60}$	$T_{60} \rightarrow T_{80}$	$T_{80} \rightarrow T_{100}$
(a) $PF_{T_i \rightarrow T_j}^{\mu^*}$	6.9	4.9	4.7	4.8	5.1	4.1	4.4
(b) $PF_{T_i \rightarrow T_j}^{\chi^*}$	4.9	4.6	2.4	2.4	2.8	2.6	2.4

## Disclosure Of Potential Conflict-Of-Interest

We wish to confirm that:

- All authors have participated in (a) conception and design, or analysis and interpretation of the data; (b) drafting the article or revising it critically for important intellectual content; and (c) approval of the final version.
- This manuscript has not been submitted to, nor is under review at, another journal or other publishing venue.
- The authors have no affiliation with any organization with a direct or indirect financial interest in the subject matter discussed in the manuscript

Signed by all authors as follows:

nia

Ines Doua-

Sofiane Boudaoud

Jéeémy Laforêt